Application of AFCM method on lap joint using low energy arc welding technologies

Saiful Din Sabdin[1,*], Nur Izan Syahriah Hussein[1], Mohammad Kamil Sued[1], Rashdan Awang[2]

1) Fakulti Kejuruteraan Pembuatan, Universiti Teknikal Malaysia Melaka,
Hang Tuah Jaya, 76100 Durian Tunggal, Melaka, Malaysia
2) TWI Technology (S.E. Asia) Sdn Bhd, No.1 Jalan Utarid U5/13 Section U5,
40150 Shah Alam , Selangor Darul Ehsan, Malaysia

*Corresponding e-mail: saifulkdh@yahoo.com

ABSTRACT – Low energy arc welding is one of the modern technologies joining of GMAW process. Commonly inspections technique is used in manufacturing and industrial which the processes involved meett those requirements especially in welding technology field. The main objective from this experiment is to identify the defect from thin plate sheet joining lap joint in relation to heat input on high strength steel plate joint. The study of this paper covers only the inspection effects using ACFM (Application of Alternating Current Field Measurement) method on the weldment low arc technology after cooling down to room temperature.

1. INTRODUCTION

Nowadays the ACFM technique mostly used at manufacturing industries such as automotive, maritime, oil & gas, aerospace and other applications. Significantly, the ACFM is from conventional eddy currents and locally used unidirectional and constant electric field in the sample. This method provides a number of benefits including the ability to mathematically model the perturbations produced by a simple defect. The technique therefore allows crack and depth sizing is needed to be carried out by comparing measured field disturbances to predict disturbances around pre-defined defects. The technique was originally developed for the detection and sizing of fatigue cracks, which tend to be single planar defects compatible with the model [1-2].

Low energy arc technology was a short circuit which sends a signal that retracts the welding filler material, giving the weld time to cool before each drop is placed. This leaves a smooth weld that is stronger than that of a hotter weld. This works well on thin metal that is prone to warping and the weld burning through the material. This type of welding is more efficient than other GMAW methods when the metal is thinner than 10mm, anything greater than the expense begins to overcome traditional welding.

2. METHODOLOGY

The Alternating Current Field Measurement (ACFM) technique is an electromagnetic technique that is capable of both detecting and sizing (length and depth) surface breaking cracks in metals. Figure 1 shows the signal basis of the technique which is constantly alternating current tangential solenoid that remote from the test surface. Inducing current electric in the sample surface is to be done to create unidirectional and uniform strength over a localized area under the solenoid. When there are no defects present in this area, this current electric will be undisturbed. Here, if a crack is present, the uniform current is disturbed, and it will flow around the ends and down the faces of the crack.
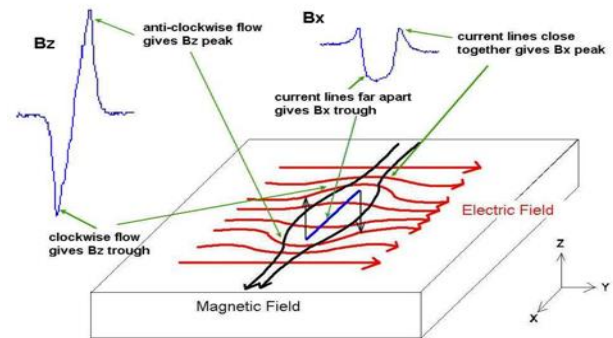

Figure 1 ACFM currents flowing around a defect and signals from scan along the defect

The experiments were conducted according to the information welding parameter in table 1. The robot welding used in this study was KUKA type KRC4 and the system is equipped by EWM ColdArc power source [3]. Specimens dimension with dissimilar thickness of 250 mm × 50 mm x 1.0 mm and 250 mm x 50 mmx 0.8 mm were fabricated. The material plate is high strength steel on lap joint [4]. The chosen parameters for the pprocess is bead-on-plate and the experiments are performed and corresponding heat input values are detailed in Table 1.

Table 1 Welding Parameter

Heat input (KJ/mm)	Ampere (A)	Voltage (v)	Welding speed (mm/min)
0.026	40	6	550

3. RESULTS AND DISCUSSION

An overview of Figure 2 showed the defect signal response on welding plate. Four defects were identified on plate measurement on Figures 2(a) and 2(b) representing depth and length of defect on the highlight circle. Figure 2(c) In the presence of a defect, the butterfly loop is drawn in the screen and for manual operation the operator looks for this distinctive shape to

decide whether a crack is present or not. The biggest defect was on zone 3 the center of welding joint plate.

Figure 3 shows the measurement length and depth on signal in weld zone. The most defect on area zone 3 is the length of 148 mm and the depth of 29 mm. The lowest defect on area zone 1 is the length of 60 mm and the depth of 7 mm. The results indicate that the heat input is affected from the weldment size. Interestingly, there were also differences correlated with the results obtained by previous researchers [5].

Table 2 shows the visual defect by zone. Visual examination showed that unequal cladding of the welding joints occurred. According to ISO 5817 which is the standard quality for the welding, welded joints can be classified according to uniform and regular joint EN ISO 5817. The results obtained was actual throat is more than design throat of fillet weld lap joint.
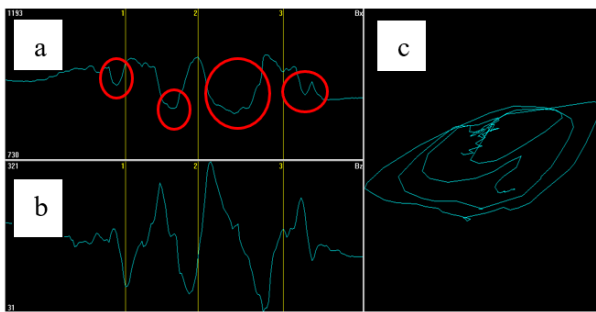

Figure 2 Signal response to defect
a) B_x signal of depth plate 200 mm, b) B_z signal of length plate 200 mm and c) signal butterfly plot.
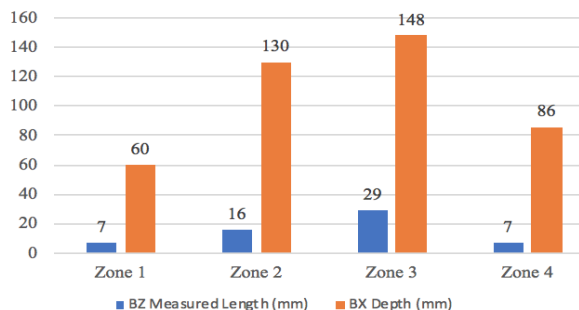

Figure 3 Graph measurement zone area.

From the experiment results there are four defects on the join using ACFM equipment more easily and accurately. The defect on weldment join is incomplete fusion and the underfill was noted. The AFCM method process proves to be suitable for inspection welding thin sheet metal. It is essential to determine the right parameter to minimize defect in the product.
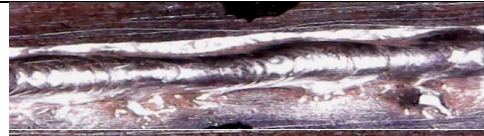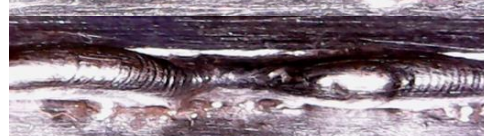
4. CONCLUSION

The most significant findings from this study is that The AFCM method is relevant to experiment and investigate thin plate defect. After completing this work, several conclusions are made from the results shown above.

(a) ACFM has been shown to be effective for inspection of simulated surface breaking geometrical defects and electromagnetic discontinuities in high strength steel plates.

(b) The technique has also obtained good results in thin skin application with higher accuracy.

(c) The technique has also inspected through coatings, making it a useful and adaptable inspection technique for the new millennium.

Table 2 Visual defect zone area.

Defect area	Zone
	1
	2
	3
	4

REFERENCES

[1] Ge, J., Li, W., Chen, G., Yin, X., Wu, Y., Yuan, X., & Zhao, M. (2016). New parameters for the ACFM inspection of different materials. *Insight-Non-Destructive Testing and Condition Monitoring*, *58*(6), 313-317.

[2] Farrell, S. P., Lugg, M., & Avery, K. (2015, March). Application of Alternating Current Field Measurement for Determination of Surface Cracks and Welds in Steel Structures at Lift-off. In *ASNT 24th Research Symposium 2015* (pp. 24-28).

[3] Sabdin, S. D., Hussein, N. I. S., Sued, M. K., & Ayof, M. N. (2018). Joining of Thin Plates Using Various Arc Welding Heat Sources–A Review. *Journal of Advanced Manufacturing Technology (JAMT)*, *12*(1(1)), 357-370.

[4] Sabdin, S. D., Hussein, N. I. S., Sued, M. K., Ayof, M. N., Ayob, M. S., & Rahim, M. A. S. A. (2018). Weld bead reinforcement on cold rolled carbon steel sheet joint using ColdArc technology. *Proceedings of Mechanical Engineering Research Day 2018*, 197-198.

[5] Ge, J., Li, W., Chen, G., Yin, X., Wu, Y., Yuan, X., & Zhao, M. (2016). New parameters for the ACFM inspection of different materials. *Insight-Non-Destructive Testing and Condition Monitoring*, *58*(6), 313-317.

Thermal degradation study of acrylonitrile butadiene styrene (ABS) composites for FFF

Syaza Najwa Mohd Farhan Han[1], Mastura Mohammad Taha[2,3,*], Muhd Ridzuan Mansor[1,3], Muhammad Mufqi Aminallah[2]

[1] Fakulti Kejuruteraan Mekanikal, Universiti Teknikal Malaysia Melaka, Hang Tuah Jaya, 76100 Durian Tunggal, Melaka, Malaysia

[2] Fakulti Teknologi Kejuruteraan Mekanikal dan Pembuatan, Universiti Teknikal Malaysia Melaka, Hang Tuah Jaya, 76100 Durian Tunggal, Melaka, Malaysia

[3] Centre for Advanced Research on Energy, Universiti Teknikal Malaysia Melaka, Hang Tuah Jaya, 76100 Durian Tunggal, Melaka, Malaysia

*Corresponding e-mail: mastura.taha@utem.edu.my

Keywords: ABS composites; thermal degradation; fused filament fabrication

ABSTRACT – Thermal stability of material is the main concern in producing filament for FFF. Hence, this paper investigates thermal stability of commercialized ABS filament, neat ABS, kenaf fiber, 2.5% and 5% of kenaf fiber reinforced ABS composites. TGA test was performed to measure the degradation temperature. Results indicate that the degradation temperature for commercialized ABS filament, neat ABS and kenaf fiber are 345.16°C 326.83°C and 240.53°C respectively. Meanwhile, addition of kenaf fiber into ABS polymer decreased the thermal stability of composites. Therefore, kenaf fiber reinforced ABS composites is suitable for FFF since extrude temperature used at FFF is less than 250°C.

1. INTRODUCTION

Fused Filament Fabrication (FFF) is the most significant technique for Additive Manufacturing (AM) and has been used widely based on the capability of FFF to print three-dimensional objects. Besides, FFF can fabricate geometrically complex shape [1] and cost-effectiveness [2] in producing 3D objects with good resolution output.

Thermoplastic is the mainly used material for FFF such as Acrylonitrile Butadiene Styrene (ABS) and Polylactic Acid (PLA). Currently, wide range of material have been introduced from neat bio(polymer) to (bio)composites [3]. However, the suitability of composites material is one of the disadvantages as the compatibility between the matrix and reinforcement requires intensive research based on the temperature of materials which the melting point is not too high or not to low since the heating element of commercially available FFF can operate around 300°celsius [4].

Natural fiber reinforced polymer composites (NFRC) has been used nowadays in many applications such as automotive, aerospace and medical due to its lightweight and environmentally friendly material [5]. The disadvantage of natural fiber such as low thermal stability limits the usage of NFRC for FFF. Torrado et al. [6] investigate effect of jute fiber reinforced ABS composites on FFF and found that the high temperature of extrusion process can cause decomposition of jute fiber. Montalvo et al. [7] study on wood plastic composites (WPC) and found that the decomposition of WPC is between 300°C and 500°C. So, it is vital to study the thermal stability of NFRC before the NFRC filament is produced and extruded on FFF.

Thus, the aim of this study is to investigate the thermal degradation of commercialized ABS filament, kenaf fiber, neat ABS and different loadings of NFRC by using thermogravimetric analysis (TGA) to identify the decomposition temperature (°C).

2. METHODOLOGY

There are five types of test samples which are commercialized ABS filament, kenaf fiber, neat ABS, 2.5% kenaf fiber reinforced ABS composites and 5% kenaf fiber reinforced ABS composites.

Commercialized ABS filament was cut into 3mm length and the weight is between 5-15mg. Neat ABS and kenaf fiber is weighed to obtain 5-15mg since the material is already in a pellets and powder form respectively. Then, an internal mixture model HAAKE Rheomix OS was used to mix 2.5 wt.% kenaf powder reinforced ABS composites and 5 wt.% kenaf powder reinforced ABS composites. The mixture was mixed at 180°C with the speed 50 rpm for 12 minutes for each mixing. After the mixing of two specimens is completed. The material was crushed by a crusher machine to obtain specimens in form of granules. Then, the granules for 2.5 wt.% and 5 wt.% percent of kenaf fiber reinforced ABS composites was weighed between 5-15mg.

The model used for TGA is TGA 1 (Thermogravimetric Analyzer) of Mettler Toledo. The temperature used for all samples is 25°c to 550°c with heating rate 10°c min⁻¹ and the atmosphere used is nitrogen gas. TGA is conducted to measure the change in mass of the sample as a function of increasing temperature and the final residue yield on set of degradation temperature were recorded.

3. RESULTS AND DISCUSSION

Figure 1 shows the results of TGA curves for commercialized ABS filament, kenaf fiber, neat ABS, 2.5 wt.% kenaf fiber reinforced ABS composites and 5 wt.% kenaf fiber reinforced polymer composites.
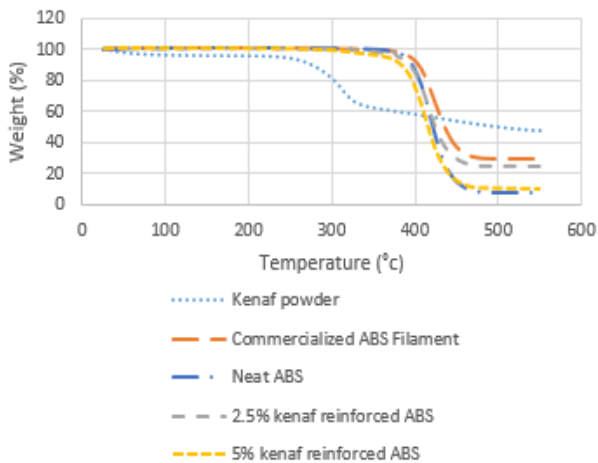
Figure 1 TGA curves for all specimen.

Table 1 Decomposition temperature and final weigh after decomposition of all specimen.

Materials	Decomposition temperature (°C)	Final weight after decomposition (%)
Kenaf powder	240.53	8.36
Commercialized ABS filament	345.16	4.6
Neat ABS	326.83	2.65
2.5% kenaf fiber	320.94	3.34
5% kenaf fiber	312.39	3.46

The data from curves were extracted and presented in Table 1. The commercialized ABS filament decomposition temperature and remaining weight is slightly higher compare to neat ABS with 5.6% and 38% respectively. Then, neat ABS have the higher decomposition temperature compare to 2.5% and 5% of kenaf fiber reinforced ABS composites.

Meanwhile, it is found that the thermal stability of kenaf fiber is the lowest with 240.53°C respectively for decomposition temperature. The overall weight loss of kenaf fiber could be divided into three different steps. For the first step, weight loss occurs at below 100°C about 6% from initial weight. Then, the second weight loss occurred around 260°C with 12.5% where this is the initial stage of thermal degradation. The last step is referred to the major thermal degradation occur with maximum weight loss at 325°C. The weight loss occurs due to the vaporization from fiber and decomposition of cellulose [8].

As the content of kenaf fiber is increased, the decomposition temperature of composites is decreased since kenaf fiber has low thermal stability compare to ABS polymer. This result is supported by Azwa and Yousif [9] where the addition of natural fiber in composites cause the thermal stability to reduce due to the less stable fibers. The increasing percentage of fiber lower the thermal stability due to weaken hydrogen bonding and the decreases of mobility cellulose chains in cellulose [10].

4. CONCLUSION

In conclusion, the degradation temperature of commercialized ABS filament is higher than neat ABS. Besides, the thermal stability of kenaf fiber was significantly lower than commercialized ABS filament and neat ABS, so the increasing content of kenaf fiber in reinforced ABS composites can reduced the thermal stability of the composites. Therefore, 2.5% and 5% of kenaf fiber reinforced ABS composites can be used as filament in FFF since the extrude temperature use at 3D printer is less than 250°C.

REFERENCES

[1] MacDonald, E., & Wicker, R. (2016). Multiprocess 3D printing for increasing component functionality. *Science*, 353(6307).

[2] Noorani, R. (2006). *Rapid prototyping: principles and applications*. John Wiley & Sons Incorporated.

[3] Le Duigou, A., Castro, M., Bevan R., & Martin, N. (2016). 3D printing of wood fibre biocomposites: From mechanical to actuation functionality. *Materials & Design*, 96, 106-114.

[4] Salem Bala, A., & bin Wahab, S. (2016). Elements and materials improve the FDM products: A review. In *Advaced Engineering Forum*, 16, 33-51.

[5] Ramamoorthy, S. K., Skrifvars, M., & Persson, A. (2015). A review of natural fibers used in biocomposites: plant, animal and regenerated cellulose fibers. *Polymer reviews*, 55(1), 107-162.

[6] Torrado, A. R., Shemelya, C. M., English, J. D., Lin, Y., Wicker, R. B., & Roberson, D. A. (2015). Characterizing the effect of additives to ABS on the mechanical property anisotropy of specimens fabricated by material extrusion 3D printing. *Additive Manufacturing*, 6, 16-29.

[7] Montalvo, J. I., & Hidalgo, M. A. 3D printing with natural reinforced filaments. In *Solid Freeform Fabrication (SFF) Symposium*, 922-934.

[8] Fauzi, F. A., Ghazalli, Z., Siregar, J. P., & Tezara, C. (2016). Investigation of thermal behaviour for natural fibers reinforced epoxy using thermogravimetric and differential scanning calorimetric analysis. In *MATEC Web of Conferences*, 78.

[9] Azwa, Z. N., & Yousif, B. F. (2013). Thermal degradation study of kenaf fiber/epoxy composites using thermo gravimetric analysis. In *Proceeding of the 3rd Malaysian Postgraduate Conference (MPC 2013)*, 256-264.

[10] Aji, I. S., Zainudin, E. S., Khalina, A., Sapuan, S. M., & Khairul, M. D. (2011). Thermal property determination of hybridized kenaf/PALF reinforced HDPE composite by thermogravimetric analysis. *Journal of thermal analysis and calorimetry*, 109(2), 893-900.

Pinless friction stir welding for weld thin plate cold rolled steel sheet

Muhammad Aizat Mohd Abd Wahab[1], Mohammad Khairul Azmi Mohd Kassim[2], Mohammad Kamil Sued[2,3,*],
Shikh Ismail Fairus Shikh Zakaria[1], Siti Noor Najihah Mohd Nasir[2]

[1] Fakulti Teknologi Kejuruteraan Mekanikal Pembuatan, Universiti Teknikal Malaysia Melaka,
Hang Tuah Jaya, 76100 Durian Tunggal, Melaka, Malaysia
[2] Fakulti Kejuruteraan Pembuatan, Universiti Teknikal Malaysia Melaka,
Hang Tuah Jaya, 76100 Durian Tunggal, Melaka, Malaysia
[3] Advance Manufacturing Centre, Universiti Teknikal Malaysia Melaka,
Hang Tuah Jaya, 76100 Durian Tunggal, Melaka, Malaysia

*Corresponding e-mail: kamil@utem.edu.my

Keywords: Pinless friction stir welding; process Parameter; SPCC

ABSTRACT – Pinless Friction Stir Welding provides various advantages in designing tool compared to the traditional Friction Stir Welding such as simple fixtures and simpler tool. The relationship of parameters is investigated by conducting a mechanical testing at the welded workpieces. Temperature distribution and current consumption during welding are recorded. Two set of parameters used which are 900rpm and 1050rpm for rotational speed; 45mm/min and 75mm/min for welding speed. It shows that lower rotational speed with higher welding speed is producing a higher strength weld which 132.34 MPa for tensile and around 150 HV for microhardness. This technique are highly recommended for aerospace application since having higher strength.

1. INTRODUCTION

Welding is a permanent process that joining two or more parts by application of heat and pressure [1]. New solid-state welding has been derived from Conventional Friction Stir Welding (CFSW) which are Pinless Friction Stir Welding (PFSW) [2]. In PFSW, tool design was an important characteristic since it produces a uniformity of welding joint. Furthermore, PFSW let the tool design to be in various type of design since different type of tool design produced a different heat during welding [3]. If the metal flow is inconsistent or inadequate heat during process, it leaded to the defects produce in welding structure [4]. Basically, the application of pin in FSW are resulting undesirable keyhole at welded area. The existed of keyhole are inviting the corrosion at the welded part [5]. Once the corrosion occurred at the welded area, it reduced the weld strength.

2. METHODOLOGY

Type of material used in this study was Cold Rolled Carbon Steel Sheet (SPCC) with 1mm thickness. The SPCC sheet are 174mm in length with 140mm for width. While for pinless tool, it was fabricate using tool steel, H13. The dimension of the tool just consists of shoulder and tool holder which are 10mm for shoulder diameter and 20mm for tool holder diameter. To make sure all the experiments are run smoothly, 3-axis Haas CNC Milling machine has been applied as the FSW machine. During this study, various of parameter are applied. However, there is certain parameter from preliminary test that give an acceptable weld product. Table 1 shows the parameter that selected for this study.

Table 1 Parameter setup based on preliminary test.

Experiment	Rotational speed (rpm)	Welding speed (mm/min)
Run 1	900	45
		75
Run 2	1050	45
		75

During PFSW process, data of temperature and current are recorded. For the mechanical testing, tensile and microhardness test were conducted. Testing are running following ASTM E8 for tensile and ASTM E384 for microhardness. Maximum loaded used was 2kg with 10s of dwell time.

3. RESULTS AND DISCUSSION

Figure 1 and 2 shows the surface appearance after running PFSW process. It shows the excessive of flash at weld area. This happened due to the outflow of the plasticized material that are underneath of the shoulder. Furthermore, an insufficient heat during welding making the process occur below the required temperature. By looking at the welded area, there is a dark colour due to the heat during welding process. However, the dark colour is ununiform since thin plate are use in this study. Therefore, the contact between pinless tool and workpiece are not uniform. Moreover, by applying thin material for this study, it was hard to get a smooth weld result since thin material are easily to distort once having higher temperature.
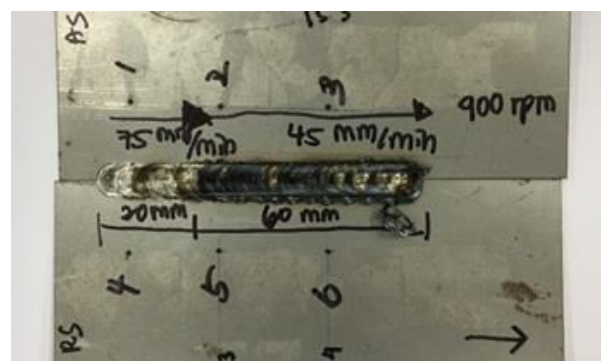

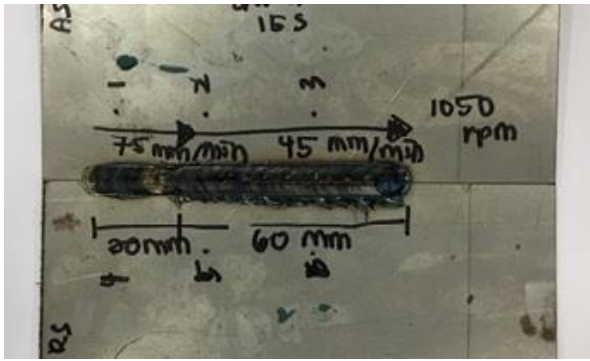Figure 1 Visual inspection of this study; 900rpm with 75mm/min and 45mm/min.

Figure 2 Visual inspection of this study; 1050rpm with 75mm/min and 45mm/min.

Table 2 represent the result of tensile test for this study. Based on the result recorded, it shows that parameter applied give a huge influence for this study. Moreover, higher welding speed are resulting to the higher tensile strength. It was stated that the tensile strength is improve by increasing of welding speed. However, the result recorded are still below from the base material resulted. It believed that stirring effect affected the arrangement of particle inside the material. It was stated that the stirring of particle that including heat are changes the arrangement of the particle inside the material.

Table 2 Results of tensile strength.

Experiment	Rotational speed (rpm)	Welding speed (mm/min)	Tensile strength (MPa)
Base Material	-	-	194.04
Run 1	900	45	93.85
		75	132.34
Run 2	1050	45	34.04
		75	118.24

Figure 3 and 4 showing a similar pattern which are the welded area having higher hardness value. The hardness value decreased when the data recorded far from welded area. This are because of the heat that produced during process that make the welded area more solid. Once the heat and force are focus on one spot, it will improve the hardness.
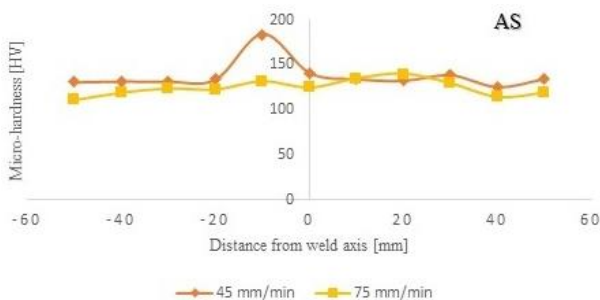

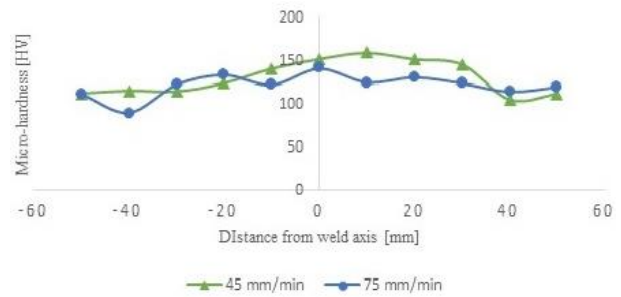Figure 3 Micro-hardness result; 900 rpm with 45mm/min and 75mm/min.

Figure 4 Micro-hardness result; 1050rpm with 45mm/min and 75mm/min.

However, there is flash at the welded part. This are because of the outflow of material underneath the shoulder due to the high plunging tool depth. Next, the surface groove produced because of the abnormal stirring since there is only flat surface at the shoulder.

4. CONCLUSION

Based on the result achieved, it shows that lower rotational speed with a higher welding speed are giving higher welding strength based on the tensile and micro-hardness test. There is still some defects showing in the welded product such as flash surface groove. Next, a good heat generated during process will produced a good quality of welding product.

REFERENCES
[1] Leitao, C., Emílio, B., Chaparro, B. M., & Rodrigues, D. M. (2009). Formability of similar and dissimilar friction stir welded AA 5182-H111 and AA 6016-T4 tailored blanks. *Materials & Design*, *30*(8), 3235-3242.
[2] Liu, Z., Cui, H., Ji, S., Xu, M., & Meng, X. (2016). Improving joint features and mechanical properties of pinless fiction stir welding of alcald 2A12-T4 aluminum alloy. *Journal of Materials Science & Technology*, *32*(12), 1372-1377.
[3] Godiganur, V. S., & Biradar, S. (2014). Comparison of friction stirs welding technique with conventional welding methods. *International Journal of Research in Engineering and Technology*, *3*, 572-6.
[4] Tan, C. W., Jiang, Z. G., Li, L. Q., Chen, Y. B., & Chen, X. Y. (2013). Microstructural evolution and mechanical properties of dissimilar Al–Cu joints produced by friction stir welding. *Materials & Design*, *51*, 466-473.
[5] Kuang, B., Shen, Y., Chen, W., Yao, X., Xu, H., Gao, J., & Zhang, J. (2015). The dissimilar friction stir lap welding of 1A99 Al to pure Cu using Zn as filler metal with "pinless" tool configuration. *Materials & Design*, *68*, 54-62.

Influence of process parameters on dimensional accuracy in GMAW based additive manufacturing

Nor Ana Rosli[1], Mohd Rizal Alkahari[1,2,*], Faiz Redza Ramli[1,3], Shafizal Mat[1,3], Ahmad Anas Yusof[1,3]

[1] Fakulti Kejuruteraan Mekanikal, Universiti Teknikal Malaysia Melaka,
Hang Tuah Jaya, 76100 Durian Tunggal, Melaka, Malaysia
[2] Advanced Manufacturing Centre, Universiti Teknikal Malaysia Melaka,
Hang Tuah Jaya, 76100 Durian Tunggal, Melaka, Malaysia
[3] Centre for Advanced Research on Energy, Universiti Teknikal Malaysia Melaka,
Hang Tuah Jaya, 76100 Durian Tunggal, Melaka, Malaysia

*Corresponding e-mail: rizalalkahari@utem.edu.my

ABSTRACT – Additive manufacturing (AM) or 3D printing began to emerge as important manufacturing technology. Wire and arc additive manufacturing (WAAM) is one of the most promising among AM technologies for metallic components. Their applicability to produce fully dense metal parts and large near net shape has attracted more attention from industries. However, the most important barrier is the quality of the printed parts which prevent its wider adoption. Currently, only a few studies dedicated to the optimization of the process parameters. Thus, the presented paper studies the effect of welding voltage, travel speed and heat input on percentage difference of height.

1. INTRODUCTION

The growth of 3D printing technology is tremendously are in the extreme level. The technology offers a promising way to produce any parts with complex geometries directly from computer aided digital designs. Clearly the advantage of AM it allows the creation of internal feature that impossible to be produced using conventional processing. WAAM systems require and energy source, automatic wire feed system, computer numerical controlled gantries or robotic system [1]. The energy source used to melt the metal wire and deposition of the metal.

However, WAAM process received less attention than others AM technique. This due to unacceptable surface finish of fabricated parts and resultant poor geometrical accuracy always keep WAAM from an industrial application such as aerospace and structural industry [2]. Usually, in other to remove unwanted geometry post-processing processes such as machining are required for any components that are built by depositing a series of overlapping beads using arc welding. Upon selecting of geometrical parts, arc welding and wire feed material contributes significantly on process parameters. Therefore, wider commercial uptake with WAAM is limited by the inability to work with acceptable surface finish and geometry. Besides that, determine the parameter setting is important for the improvement of welding quality and reduction of cost. Thus, this present study explores the effect of WAAM process parameters on the geometrical characteristics of metal deposited beads. The models in view of rectangular metal deposited with size 50 mm x 10 mm x 40 mm.

2. EXPERIMENTAL SETUP

The test was performed using in house developed 3D printing system [3] which is integrated with Gas Metal Arc Welding (GMAW) as shown in Figure 1. The experiment has been carried out on a substrate of a mild steel plate of 6 mm thickness, 300 mm long and 300 mm wide. An ER 70S-6 server as a filler wire with 0.8 mm diameter coaxial along GMAW. This work used the zig-zag tool path pattern.
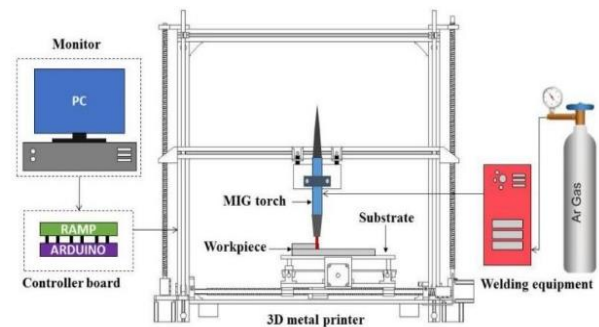

Figure 1 Experimental setup.

The process parameters involved as shown in Table 1. In order to ensure the depositing process steady, the 3D printing speed was kept in the range from 20 to 80 mm/s. The wire feed speed was set at 2800 mm/min. Welding voltage was varied from 18.5 to 22.5 V. Meanwhile, constant nozzle to plate distance, layer height and welding current were used for deposition sample, which was 5 mm, 2 mm and 100 A respectively. It should be noted that the range of parameters is designed just seldom used in practical application. A total of 9 samples were printed using varying process parameters. The first five samples with the varying voltage between 18.5 to 22.5 V were printed. Next four samples were printed by varying speed between 20 to 80 mm/s.

Table 1 Process parameters.

Parameter	Range
Travel speed, v (mm/s)	20 – 80
Wire feed speed (mm/min)	2800.
Nozzle to plate distance (mm)	5
Layer height (mm)	2
Welding current, I (A)	100
Welding voltage, V (volt)	18.5 - 22.5

3. RESULTS AND DISCUSSION

The result presented the effect of heat input on the dimensional accuracy of height weld bead deposition. The combination of welding voltage and travel speed produce significance impact on accuracy due to inappropriate heat input distribution. Figure 2 shows a graphical way of illustration the percentage of dimensional change in height due to heat input distribution at a different voltage.
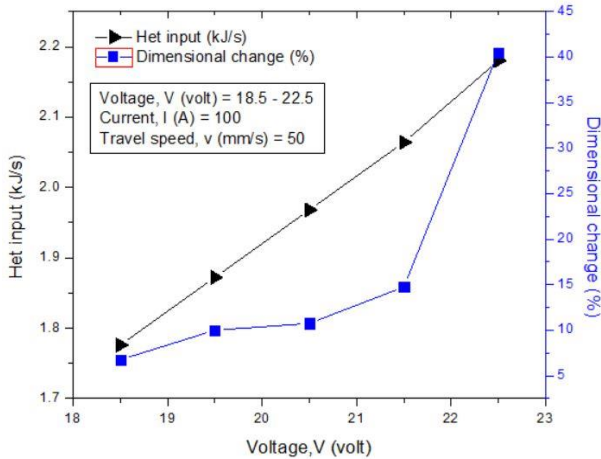

Figure 2 Relationship between the voltage, heat input and percentage of dimensional change.

It can be observed form these graphs a clear direct relation between heat input and voltage was identified. The most striking result emerges from the less heat input which produces the less dimensional change in height. The minimum percentage difference was 6.75% at 18.5V and heat input 1.776 kJ/s. These findings seem consistent with other researcher perspectives with the influence of heat input in acquired the acceptable geometrical accuracy. Suryakumar concludes the great importance for better geometric resolution is less heat input and better heat distribution [4]. Due to continued deposition with excessive heat input in the local area result in poor dimensional tolerance and surface finish. The relationship of speed, heat input, and dimensional change is indicated in Figure 3. The graph shows gradually decreasing of heat input while the travel speed is increasing.
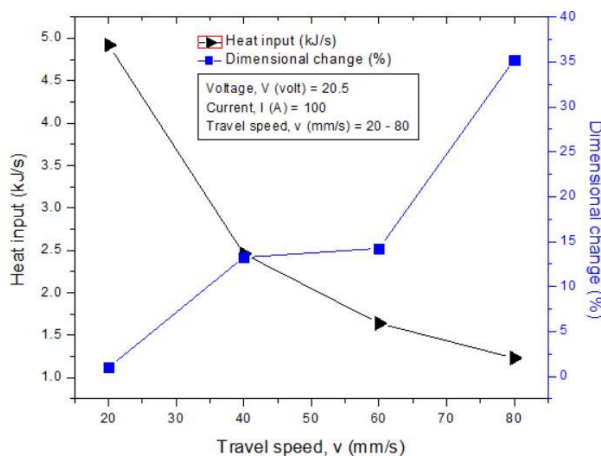

Figure 3 Relationship between the speed, heat input and percentage of dimensional change.

The minimum percentage of dimensional change is 1% and slightly decrease than former experiments. The greatest percentage difference of height about 21% at travel speed 60 mm/s to 80 mm/s. It is noticeable that, low heat input can be achieved by using higher speed. However, unacceptable geometries were found if less heat input and fast moving speed. It can be seen the height of the deposited layers decrease with an increase in travel speed. Higher speed is preferred to achieve high productivity, but it should be appropriate with the combination of others parameters. The minimum percentage difference was 1% at travel speed 20 mm/s and heat input 4.920 kJ/s as shown in Figure 4. This shows the importance of travel speed in deposition the weld bead. As the rate of travel speed reduces, the exposure time of weld beads is increasing and resulting higher heat input. Moreover, the increase of heat input found to be more prominent at high current setting. Xiongrong Li points out that high heat input is needed to achieve full penetration but fairly acceptable speed to prevent high distortion.
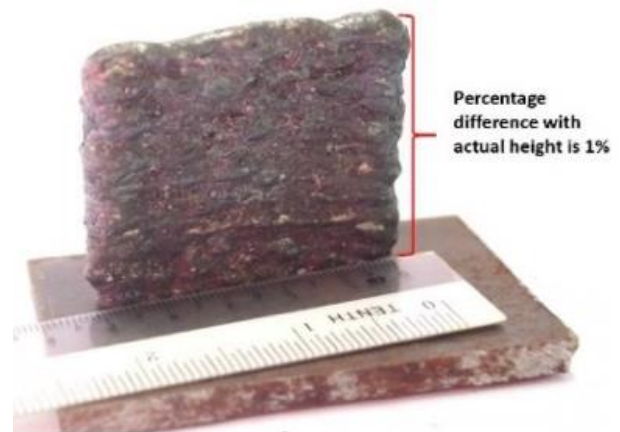

Figure 4 Sample with minimum dimensional change.

4. CONCLUSION

This study has presented an analysis of the effect of welding voltage, travel speed, heat input on percentage difference of height. Taking into account the effect of heat input, the result reveals the increasing of heat input forms excessive weld bead and produce large percentage difference than actual. Hence, it is important to optimize the parameter so that a relatively good dimensional accuracy printed part can be achieved.

REFERENCES

[1] Wu, B., Pan, Z., Ding, D., Cuiuri, D., Li, H., Xu, J. & Norrish, J. (2018). A review of the wire arc additive manufacturing of metals: Properties, defects and quality improvement. *Journal of Manufacturing Process*, *35*, 127–139.

[2] Paskual, A., Álvarez, P. & Suárez, A. (2018). Study on arc welding process for high deposition rate

additive manufacturing. *Procedia CIRP*, *68*, 358-362.

[3] Rosli, N.A., Alkahari, M.R., Ramli, F.R., Maidin, S., Sudin, M.N., Subramoniam, S. & Furumoto, T. (2018). Design and Development of a low cost 3D metal printer. *Journal of Mechanical Engineering Research & Development, 41*(3), 47-54.

[4] Suryakumar, S., Karunakaran, K.P., Bernard, A., Chandrasekhar, U., Raghavender, N. & Sharma, D. (2011). Weld bead modeling and process optimization in hybrid layered manufacturing. *Computer-Aided Design, 43*(4), 331-344.

Total volatile organic compound (TVOC) exposure from recycle polyamide nylon powder during selective laser sintering process

Amir Abdullah Muhamad Damanhuri[1,*], A. Shamsul Rahimi A. Subki[2], Azian Hariri[3],
Muhammad Hafidz Fazli Md Fauadi[4], Mohammad Rafi Omar[1], Abdul Munir Hidayat Shah Lubis[1]

[1] Fakulti Teknologi Kejuruteraan Mekanikal dan Pembuatan, Universiti Teknikal Malaysia Melaka,
Hang Tuah Jaya, 76100 Durian Tunggal, Melaka, Malaysia
[2] Fakulti Teknologi Kejuteraan Elektrik dan Elektronik, Universiti Teknikal Malaysia Melaka,
Hang Tuah Jaya, 76100 Durian Tunggal, Melaka, Malaysia
[3] Fakulti Kejuteraan Mekanikal dan Pembuatan, Universiti Tun Hussein Onn Malaysia,
86400, Parit Raja, Bt Pahat, Johor, Malaysia
[4] Fakulti Kejuteraan Pembuatan, Universiti Teknikal Malaysia Melaka,
Hang Tuah Jaya, 76100 Durian Tunggal, Melaka, Malaysia

*Corresponding e-mail: amir.abdullah@utem.edu.my

Keywords: Total volatile organic compound; selective laser sintering; exposure

ABSTRACT – Polyamide nylon (PA12) is semi crystalline polymers that are common materials use in selective laser sintering (SLS) process. Usually, unsintered powder will be recycled to used back for SLS printing. Therefore, this study investigates the exposure of total volatile organic compound (TVOC) from recycle polyamide nylon during SLS printing process. Prior to the investigation, the recycle powder was sent for thermogravimetric analysis (TGA). Calibration block was set to be print SLS machine, filled with 30kg of powder. Real time sampling was accordingly to Industry Code of Practice by DOSH Malaysia for 8 hours indoor sampling. TGA revealed that no composition loss during normal sintered temperature. The highest TVOC emission present at post printing process (powder cake breakout) of 1.7ppm. Mitigation strategies are suggested to reduced occupational exposure of TVOC emission to the SLS operators.

1. INTRODUCTION

Nowadays, 3D printer is now a common machine to general public due to its rapid prototyping. Military, medical devices, aerospace and automotive are fields that use additive manufacturing (AM) of 3D printer to print their prototype and products. There are several type of AM categories such as photo polymerization, material extrusion, powder bed fusion, direct energy deposition, sheet lamination, material jetting, and binder jetting. Selective laser sintering meanwhile includes in the category of powder bed fusion [1]. Polymers powder especially polyamide nylon are common material used in SLS. During SLS printing process, only powder which heated by the scanning action will crystallize to become the final product, and others remain and turn to recycled powder. However, the use of these powder in nontraditional manufacturing environments may pose health risks to group of people that are handling SLS printing process. AM machine can release volatile organic compounds chemical and particles into air while printing processes [2]. They are not built with air cleaning system; the situation could be worst if use in an enclosed space without proper air flow or ventilation. Studies show that VOC have negative impacts on human

and environmental health [3]. Therefore, this study aims to investigates the exposure of total volatile organic compound (TVOC) during 3D printing of SLS process from recycle powder of polyamide nylon (PA12).

2. METHODOLOGY

The recycle polyamide nylon powder were collected from SLS Laboratory Fakulti Teknologi Kejuteraan Mekanikal dan Pembuatan, FTKMP of Universiti Teknikal Malaysia Melaka (2°16'40.4"N 102°16'32.4"E).The powder has been heated 172 °C laser temperature during 3D printing previously. Prior to the exposure analysis, the recycle powder were sent for Thermogravimetric Analysis (TGA) using Thermal Gravimetric Analyzer Linseis Model. Thermal analysis was conducted at room temperature until 600 °C with heating rate of 10 °C/min. The SLS 3D printer use for this project is Farsoon SS402P that operated with scanner of dynamic focusing, high accuracy galvo scanning system. The machine has external dimension size of 2660mm x 1540mm x 2150mm with weight of 3000 kg. The maximum printing prototype are 350 mm x 350 mm x 350 mm with capacity of 60kg powder. The type of laser is carbon dioxide (CO_2) with 100W power, and laser wave length is 0.3 mm with scanning speed of 12.7 m/s. The thickness of powder layer for every rotating roller pass through was set to be 0.2mm. The sintered temperature of powder chamber was set to 190°C. Calibration block with dimension of 56 mm X 56 mm and 9 mm thickness was set to be print with 30kg of recycle powder [4]. The TVOC emission monitoring from SLS printing process divided into four phases [5], where: a) pre-printing, b) powder preparation (mixing powder), c) printing, and d) post printing.

Indoor sampling was perform in SLS Laboratory of FTKMP accordingly to DOSH Malaysia Indoor Air Quality Code of Practice (ICOP DOSH 2010) [6]. The laboratory was divided into two rooms as depicted at Figure 1. To measure the TVOCs, a ppbRAE monitor (ppbRAE 3000, USA, RAE System Inc) was used for real time sampling of 8 hours printing process. The instrument set to be 1 meter from floor, at 5 minutes
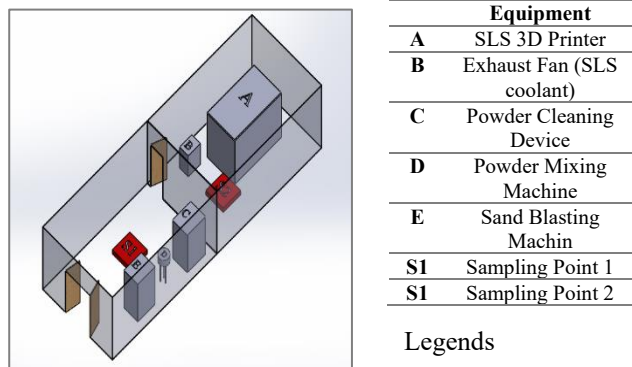
interval sampling.

	Equipment
A	SLS 3D Printer
B	Exhaust Fan (SLS coolant)
C	Powder Cleaning Device
D	Powder Mixing Machine
E	Sand Blasting Machin
S1	Sampling Point 1
S1	Sampling Point 2

Legends

Figure 1 SLS Laboratory and sampling locations.

3.   RESULT AND DISCUSSION

Thermogravimetry analysis (TGA) and Difference Thermo Gravimetry (DTG) are plotted in Figure 2. TGA present several step of mass loss from recycle polyamide nylon namely (i) at temperature around 300ºC, a low level of water absorption which is about 10% was observed, (ii) at around 300ºC to 400ºC with another 10% loss, (iii) at around 400ºC to 480ºC, corresponds to the most important mass loss during thermal decomposition and (iv) final mass loss at 550ºC [7].
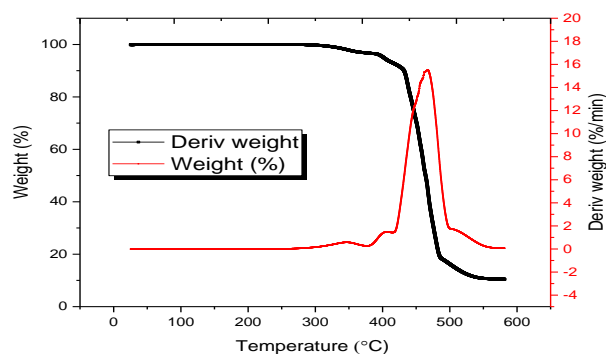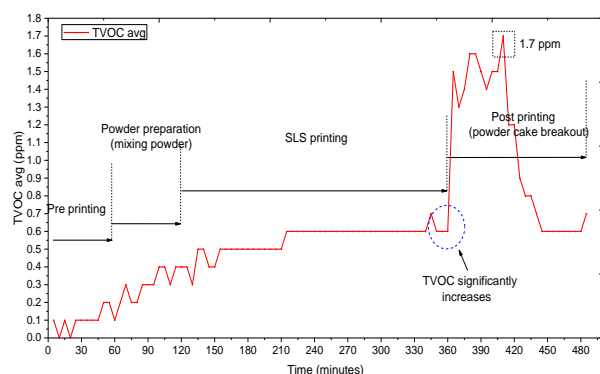

Figure 2 TGA and DTG analysis.

Figure 3 TVOC exposure during SLS printing process.

The emission of TVOC from SLS printing process were depicted at Figure 3. The TVOC slowly increase during preparation powder phase and maintain at a constant amount during SLS printing prototype. However, the emission gradually increases and at 360 minutes, where powder cake was taken out from SLS chamber for powder cake breakout phase and same

agreement with Preez S.D. et al,.[5]. The TVOC shows highest value of emission at 410 minutes (1.7ppm). The influence of powder cake temperature significantly increase the emission of TVOC [3].

4.   CONCLUSION

In this study, the TVOC emission from recycle polyamide nylon (PA12) was present. The TGA analysis shows there was no significant amount of thermal composition lost at normal sintered temperature (200 °C). Meanwhile, the TVOC emission hit the highest value during post printing process. The emission increases slowly at the beginning of process, and stable during SLS printing phase. The present of TVOC emission during SLS printing process shows potential health hazard to the operators. Mitigation strategies such ventilation and suitable personal protective equipment are necessary to make sure operators works in safe environment.

REFERENCE
[1]   Prakash, K. S., Nancharaih, T., & Rao, V. S. (2018). Additive Manufacturing Techniques in Manufacturing-An Overview. *Materials Today: Proceedings*, *5*(2), 3873-3882.
[2]   Azimi, P., Zhao, D., Pouzet, C., Crain, N. E., & Stephens, B. (2016). Emissions of ultrafine particles and volatile organic compounds from commercially available desktop three-dimensional printers with multiple filaments. *Environmental Science & Technology*, *50*(3), 1260-1268.
[3]   Damanhuri, A. A. M., Leman, A. M., Abdullah, A. H., & Hariri, A. (2015). Effect of toner coverage percentage and speed of laser printer on total volatile organic compound (TVOC). *Chemical Engineering Transactions*, *45*, 1381-1386.
[4]   Afshar-Mohajer, N., Wu, C. Y., Ladun, T., Rajon, D. A., & Huang, Y. (2015). Characterization of particulate matters and total VOC emissions from a binder jetting 3D printer. *Building and Environment*, *93*, 293-301.
[5]   Du Preez, S., Johnson, A., LeBouf, R. F., Linde, S. J., Stefaniak, A. B., & Du Plessis, J. (2018). Exposures during industrial 3-D printing and post-processing tasks. *Rapid Prototyping Journal*, *24*(5), 865-871.
[6]   [6] DOSH Malaysia. (2010). Industry code of practice on indoor air quality 2010, JKKP DP (S) 127/379/4-39. 1-50.
[7]   Chen, P., Wu, H., Zhu, W., Yang, L., Li, Z., Yan, C., ... & Shi, Y. (2018). Investigation into the processability, recyclability and crystalline structure of selective laser sintered Polyamide 6 in comparison with Polyamide 12. *Polymer Testing*, *69*, 366-374.

Factors for increasing additive manufacturing (3D printing)

Ai Nurhayati[*], Ahmad Rivai, Rina Indrayani

Faculty of Industrial Engineering, Sekolah Tinggi Teknologi Bandung, Soekarno-Hatta, 378 Bandung, Indonesia

[*]Corresponding e-mail: ain38375@gmail.com

Keywords: 3D printing; analysis factors; SPSS

ABSTRACT – 3D printing is needed in the industrial world, especially for prototyping. The problem found is that the product results are not as expected by consumers. The purpose of this research is to find out what factors can improve 3D printing products to meet user expectations. This research uses factor analysis method with SPSS version 25 software to find out factors that can improve 3D printing products. The results of the analysis show that the output material factor of 3D printing is the main factor for the improvement of 3D printing products.

1.   INTRODUCTION

Additive manufacturing is often referred to as 3D printing. There are several general steps in the 3D printing process. The generic Additive Manufacturing (AM) process is [1]:

  (a) Step 1: CAD
  (b) Step 2: Conversion to STL
  (c) Step 3: Transfer to AM machine and STL File Manipulation
  (d) Step 4: Machine Setup
  (e) Step 5: Build
  (f) Step 6: Removal
  (g) Step 7: Post-processing
  (h) Step 8: Application

The consumption growth rate of 3D printing is increasing year by year as shown in Figure 1. The level of 3D printing needs is predicted to continue to rise to reach $ 21 billion by 2020 in the international world. This is a good opportunity for Indonesia to be able to increase 3D printing manufacturers in the country of Indonesia.
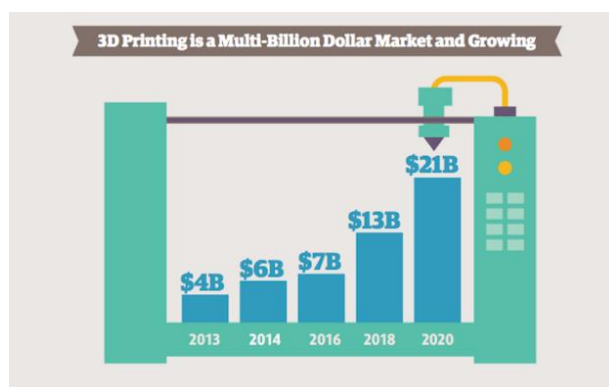

Figure 1 The growth rate of 3D printing [2].

The majority of the use of 3D printing in the world is to make prototypes by 55% as shown in Figure 2. The department that most often uses 3D printing is the research and development department as shown in Figure 3.
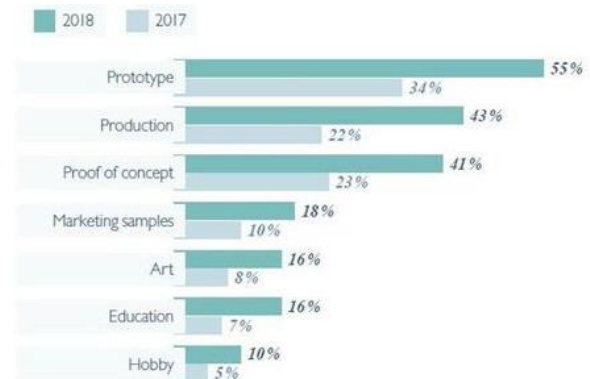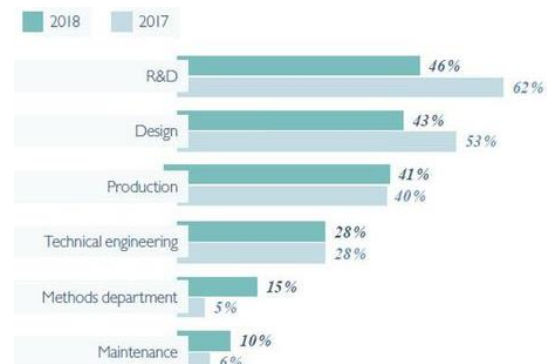

Figure 2 3D printing applications [3].

Figure 3 3D printing users by the department [3].

3D printing is very attractive to the Indonesian people, especially for the purpose of making prototypes. The problem found is that the product results are not as expected. The problem is to find out what factors can improve 3D printing products in order to meet the expectations of the Indonesian people. 3D printing manufacturers need to know what factors need to be improved in developing 3D printing products to be useful in accordance with customer expectations. The purpose of this research is to find out what factors can improve 3D printing products to meet user expectations. Several factors were considered in focus group discussions that could affect the performance improvement of 3D printing products. There are 8 factors as follows: time, cost, quality, material, effect, simple, easy to use, and color. In this study using the factor analysis method through the SPSS version 25 software program.

2.   METHODOLOGY

Factor analysis is a statistical method used to describe variability among observed, correlated variables in terms of a potentially lower number of unobserved variables called factors. Factor analysis is a multivariate

analysis method used to group large numbers of variables into a small group of variables. The aim of all factor analytic techniques is to explain patterns of covariation among observed variables using unobserved constructs [4]. Factor analysis is one method that is useful for establishing evidence for validity [5]. Factor analysis method allows us to describe many variables using a few factors. This method helps us to select a small group of variables of representative variables from a larger set. In factor analysis we represent the variables $y_1, y_2,.., y_p$ as linear combinations of a few random variables $f_1, f_2,... , f_m$ ($m < p$) called factors [6]. Factor analysis decision process [7]:

(a) The objective of factor analysis
(b) Designing a factor analysis
(c) Assumptions in factor analysis
(d) Deriving factors and assessing the overall fit
(e) Interpreting the factors
(f) Validation of factor analysis
(g) Additional uses of factor analysis results.

The use of factor analysis is widespread; examples can be found in highly ranked journals in many disciplines, including industrial engineering, economics, and manufacture [8]. The method used in this study is factor analysis using SPSS version 25 software.

3. RESULTS AND DISCUSSION

Based on the results of interviews and field surveys that are discussed and considered in focus group discussions, there were 8 variables that influenced the improvement of 3D printing tools. These variables are time, cost, quality, material, effect, simple, easy to use, and color. From the eight variables then processed by factor analysis method use SPSS version 25 software.

The output of the factor analysis method is presented in Table 1. The KMO value is above 0.5 and the significant number is below 0.05 which indicates that the research data can be processed further.

Table 1 KMO and Bartlett's test.

Kaiser-Meyer-Olkin measure of sampling adequacy		0,673
Bartlett's test of Sphericity	Approx. Chi-Square	34,782
	Df	6
	Sig.	0,000

The results obtained that there are four variables that influence the improvement of 3D printing products as shown in Table 2.

In Table 3, it can be seen that the components or factors are sorted from the lowest value to the highest value. The highest factor influencing the performance improvement of 3D printing tools is material factors.

Table 2 Anti-image matrices.

		Time	Quality	Output	Material
Anti-image Covariance	Time	,803	-,210	,021	-,177
	Quality	-,210	,786	-,102	-,120
	Output	,021	-,102	,688	-,312
	Material	-,177	-,120	-,312	,614
Anti-image Correlation	Time	,702a	-,264	,028	-,252
	Quality	-,264	,756a	-,138	-,173
	Output	,028	-,138	,637a	-,479
	Material	-,252	-,173	-,479	,640a

a Measures of Sampling Adequacy (MSA).

Table 3 Component matrix.

	Component
Time	0,646
Quality	0,697
Output	0,726
Material	0,817

Extraction method: Principal component analysis.

4. CONCLUSION

Based on the results of the research show that material factors are the main factors that can improve the performance of 3D printing to obtain product output that is in accordance with customer expectations.

REFERENCES

[1] Gibson, I., Rosen, D. W., & Stucker, B. (2014). *Additive manufacturing technologies* (Vol. 17). New York: Springer.

[2] Computer world: Electronic References. 3D printing industry to triple in four years to $21B. Retrieved April 30, 2019, from https://www.computerworld.com.

[3] Forbes: Electronic References. The state of 3D printing, 2018. Retrieved April 30, 2019, from https://www.forbes.com.

[4] Wright, A. G. (2017). The current state and future of factor analysis in personality disorder research. *Personality Disorders: Theory, Research, and Treatment*, *8*(1), 14.

[5] Wetzel, A. P. (2012). Factor analysis methods and validity evidence: a review of instrument development across the medical education continuum. *Academic Medicine*, *87*(8), 1060-1069.

[6] Rencher, A. C., & Christensen, W. F. (2002). Méthods of multivariate analysis. a john wiley & sons. *INC.: Toronto, ON, Canada*.

[7] Hair, J. F., Black, W. C., Babin, B. J., & Anderson, R. E. (2010). Multivariate data analysis: Global edition.

[8] Van der Eijk, C., & Rose, J. (2015). Risky business: factor analysis of survey data–assessing the probability of incorrect dimensionalisation. *PloS one*, *10*(3), e0118900.

Effects of current and wire feed direction in WAAM-TIG

Johnnie Liew Zhong Li[1], Mohd Rizal Alkahari[1,2,*], Nor Ana Rosli[1], Faiz Redza Ramli[1,3], Rafidah Hasan[1,3]

[1] Fakulti Kejuruteraan Mekanikal, Universiti Teknikal Malaysia Melaka,
Hang Tuah Jaya, 76100 Durian Tunggal, Melaka, Malaysia
[2] Advanced Manufacturing Centre, Universiti Teknikal Malaysia Melaka,
Hang Tuah Jaya, 76100 Durian Tunggal, Melaka, Malaysia
[3] Centre for Advanced Research on Energy, Universiti Teknikal Malaysia Melaka,
Hang Tuah Jaya, 76100 Durian Tunggal, Melaka, Malaysia

*Corresponding e-mail: rizalalkahari@utem.edu.my

Keywords: 3D printing; additive manufacturing; wire arc additive manufacturing (WAAM)

ABSTRACT – WAAM-TIG has many parameters affecting the fabricated structure. This paper reports the effect of current and wire feed direction on the weld bead of TIG. Detail design and experimental set up are provided. Different current values and wire speed direction are tested. The structure of specimens is tabulated, compared and analyzed. The current and wire feed direction can significantly affect the fabricated metal part. The optimal current range for this open sources TIG 3D metal printer is 75A to 85A. Front wire feedstock direction is recommended in WAAM-TIG.

1. INTRODUCTION

Wire arc additive manufacturing (WAAM) is increasingly being used worldwide due to its capabilities of reducing the cost and time. Generally, AM technology was invented to remove the limitation of traditional subtractive manufacturing (SM) [1]. There are three types commonly used heat sources used in WAAM which are metal inert gas welding (MIG), tungsten inert gas welding (TIG) and plasma arc welding (PAW) [2]. WAAM-MIG process is easier and more convenient compared to WAAM-TIG and WAAM-PAW due to its continuous wire spool with the welding torch which does not have wire feed direction problem. MIG uses a direct feeding spool system which is the MIG wire feed is coaxially with the welding torch and does not encounter the problem of wire feed angle and orientation. Unlike MIG, tungsten inert gas welding (TIG) and plasma arc welding (PAW) need an external wire feed machine to supply the additive materials. Angles and positions of the external wire feed can affect the quality and appearance of the weld bead.

TIG deposition rate is around 1kg/h [3]. TIG welding process is normally used to consolidate thin and middle-sized metal by melting it with an arc that created between non- consumable electrode and the workpiece with the existence of inert gas such as argon and helium gas. Shielding gases play a role to shelter the weld pool from being oxidized and contaminated. In this research, the effect of current and wire feed direction in TIG are studied.

2. METHODOLOGY

A 20mm×20mm of a square single line is drawn by using CATIA. The experiment was carried out on an aluminum plate. An open source 3D printing is used with CEA MATRIX 400 AC/DC TIG welder is used as the heat source. ER5356 aluminum rod is used as the feedstock. The schematic diagram of the machine setup is shown in Figure 1.
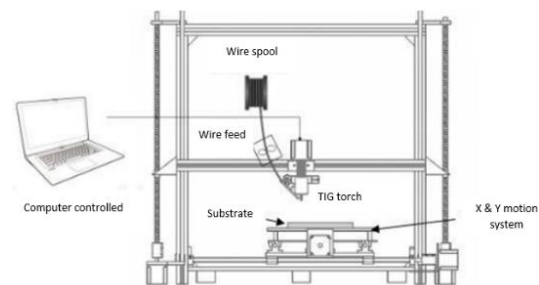

Figure 1 Schematic diagram of machine setup.

Table 1 Parameters setting.

Parameter	Unit	Values
Current	A	65 - 85
Wire feed angle	degree	45
Wire feed rate	mm/min	1200
Travel speed	mm/s	1.5
Stand-off distance	mm	5
Voltage	V	65

The machine and welding parameter are shown in Table 1. 20mm×20mm square line was printed with different current. The wire feed stock was placed on three different directions as shown in Figure 2. The sample is print from the starting point to point 1 in -ve x-direction which the wire feed is placed in front of the torch. Direction B is print from point 1 to point 2 in -ve y-direction which the wire feed is in the side position whereas direction C prints from point 2 to point 3 in +ve x-direction as the wire feed position is behind the torch. Direction D is print from point 3 to ending point which is the wire feed position is same as direction B.

3. RESULTS AND DISCUSSION

All samples were successfully fabricated. Figure 3 shows the comparison of weld bead width with different current values and directions. The molten pool size is getting larger as the current value increases and affecting weld bead width. The sample 65A and 70A produce a little droplets deposition and discontinuous deposition respectively. It was shown that the range 65A to 70A

could not melt the aluminum rod as shown in Figure 3(a) and 3(b). The continuous deposition was achieved when the current set to 75A. Unfortunately, the weld bead is overlapped in direction C in which the wire feedstock is placed behind the torch. For sample 80A, the single layer was fabricated better than sample 75A as the deposition is smooth and no defects or overlap occur in all directions. Deposition of sample 80A and sample 85A are alike but the weld bead width of the sample 85A is wider. It is because of the heat affected zone (HAZ) for sample 85A is higher than 80A. The range of HAZ is depending on the rate of heat input and the heat input increases as the current increases [4]. Thus, the width of sample 85A is wider than sample 80A. Wire feeding direction can affect the waveform and width of the single weld bead layer. The width of direction A, B, C and D for sample 80A are 6.60mm, 6.15mm, 7.61mm, and 7.98mm respectively. Direction A and B 's weld bead is more constant than direction C and D. The conditions of the welding process can be indicated through the weld bead appearance. The welding process and deposition looks stable at current 80A. However, things changed in different wire feed directions. It was obviously shown that the direction A which is the wire feed placed in front of the torch has the best weld bead appearance compares to other wire feed directions [5]. The overlap commonly occurred in the direction C which the wire feed is placed behind the torch as shown in Figure 3(c), (d) and (e).
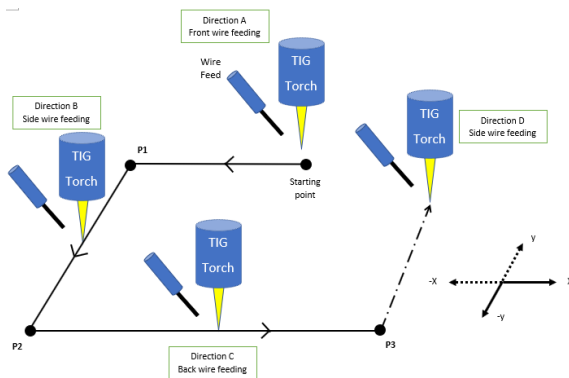

Figure 2 Wire feed direction.

Based on the results, 80A has the most satisfied weld bead appearance in direction A where the wire feed is placed in front of the torch. Thus, five layers specimen was fabricated using 80A in direction A as shown in Figure. The specimen was fabricated layer upon layer and form into a rectangular wall. The height 11mm which is 2mm taller than the CAD dimension. Inclusion and depression were found in the fabricated rectangular wall. This phenomenon occurs are generally due to the imperfection in wire especially the wire rod is twisted.

4. CONCLUSION

The current and wire feed direction can significantly affect the fabricated metal part. The optimal current range for this open sources TIG 3D metal printer is 75A to 85A. Front wire feedstock direction is recommended in WAAM-TIG. Multiple layers are possible to be fabricated with suitable parameter and it can be explored detailly in future. However, the application of TIG in WAAM requires modification on

the wire feeding system as the WAAM-TIG very much dependent on the wire position which affects its dimension accuracy.
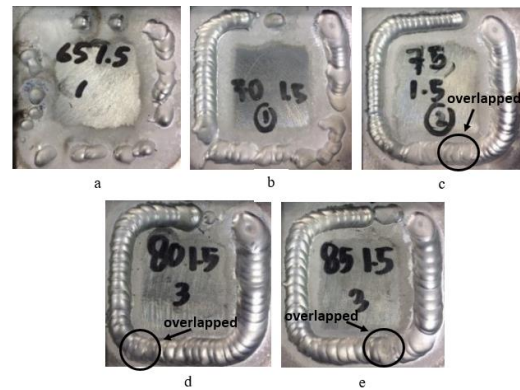

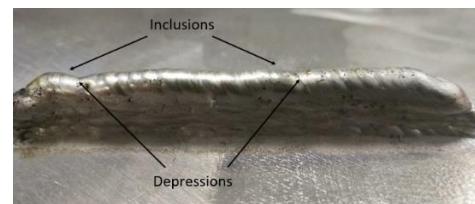Figure 3 Deposition of sample at (a) 65A, (b) 70A, (c) 75A, (d) 80A & (e) 85A.

Figure 4 Inclusion and depression occurred on five layers specimen using WAAM-TIG at 80A and Direction A (front wire feed).

REFERENCES

[1] Rosli, N. A., Alkahari, M. R., Ramli, F. R., Maidin, S., Sudin, M. N., Subramoniam, S., & Furumoto, T. (2018). Design and development of a low-cost 3D metal printer. *Journal of Mechanical Engineering Research and Developments, 41*(3), 47-54.

[2] Xiong, J., Lei, Y. Y., Chen, H., & Zhang, G. J. (2017). Fabrication of inclined thin-walled parts in multi-layer-single-pass GMAW-based additive manufacturing with a flat position deposition. *Journal of Materials Processing Technology, 240*, 397-410.

[3] Almeida, P. S., & Williams, S. (2010). Innovatie process model of Ti-6Al-4V additive layer manufacturing using cold metal transfer (CMT). *Proceeding of the 21st Annual International Solid Freeform, Unvinersity of Texas Austin.*

[4] Mamat, S., & Jamlan, S. (2015). Effect of welding heat input on microstructure and mechanical properties at coarse grain heat affected zone ABS grade a steel. *ARPN Journal of Engineering and Applied Sciences. 10*(20), 9487-9495.

[5] Ding, D. H., Pan, Z. X., Cuiuri, D., & Li, H. J. (2015). Wire-feed additive manufacturing of metal components: technologies, develpoments and future interests. *International Journal of Advanced Manufacturing Technology. 81*(1-4), 465-481.

Electromyography sensing on tibialis and peroneus muscle against improvised flat feet orthotic insole

Umi Hayati Ahmad*, Nuratifah Abdul Kudus, Mohd Hidayat Ab Rahman, Nurul Syifaa' Jamaluddin

Fakulti Teknologi Kejuruteraan Mekanikal dan Pembuatan, Universiti Teknikal Malaysia Melaka,
Hang Tuah Jaya, 76100 Durian Tunggal, Melaka, Malaysia

*Corresponding e-mail: umihayati@utem.edu.my

ABSTRACT – The objectives of this paper are to investigate the muscle activity against improvised flat feet orthotics insole using electromyography. Length, width and thickness of orthotics insole are based on average size of flat feet respondents. Flexifoam X were filled up in the fabricated wood mould. The comparison between fabricated and existing orthotics insole shows different result during evaluation using electromyography on tibialis anterior and peroneus longus generated by muscle strength responsible for lower limb movement. The different material for each insole contributes to vary result on average median frequency and root mean square that produce by the muscle from each respondent.

1. INTRODUCTION

Walking is when only one foot at a time leaves contact with the ground. According to research, the average human walks a day is about three thousand steps. Running is when both feet are off the ground with each step. Running is a method of terrestrial locomotion allowing humans to move rapidly on foot that is related to the movement of the lower limb. Brown, C. [1] stated that in 1865, Everett H. Dunbar makes a breakthrough by inventing an arch support orthotic Arch orthotics is a shoe insole that is design like the shape of an arch and it is a function to provide support or cushion to feet and help to curb pain on feet. Everett H. Dunbar inserts a layer of leather between the insole and outsole of the shoe that is shaped like an arch which resembles the shape of feet. While in 1905, Whitman Brace invents the first full foot orthotic that is made of heavy metal.

According to Bateni, H. [2] the orthotics insole can provide postural stability and reduce foot pain for the sports usage. Mercer and Horsch [3] stated that orthotic insoles can support the feet controlling abnormal for motion in order to prevent it from moving inward or outward. This study aims to improve the efficiency of the orthotic insole for flat feet focus on sports usage and measure the muscle fatigue using electromyography on tibialis and peroneus muscles.

2. METHODOLOGY

Questionnaire has been distributed among students in UTeM in order to know the population of flat feet in UTeM (N=40), the flat feet respondents amongst them are only (N=8). Morphological chart as shown in Figure 1 and concept screening were used in this study to generate suitable design for flat feet correspondent based on their requirement during survey.

Criteria	Criteria 1	Criteria 2	Criteria 3	Criteria 4
Arch Support				
Heel support				
Heel Pad				
Metatarsal support				
Heel type				
Lightweight	Light material	Minimal Part	Thin	
Aesthetic	Slim form	No Assembly	Curved Surface	Simplicity

Figure 1 Morphological chart of orthotic insole characteristic.

There are main characteristics of orthotics insole that help a person with flat feet to reduce the pain during sports activities, they are deep heel cup, heel pad, metatarsal pad, and sufficient arch support. This improvised orthotic insole is designed with standard dimensions from both male and female.
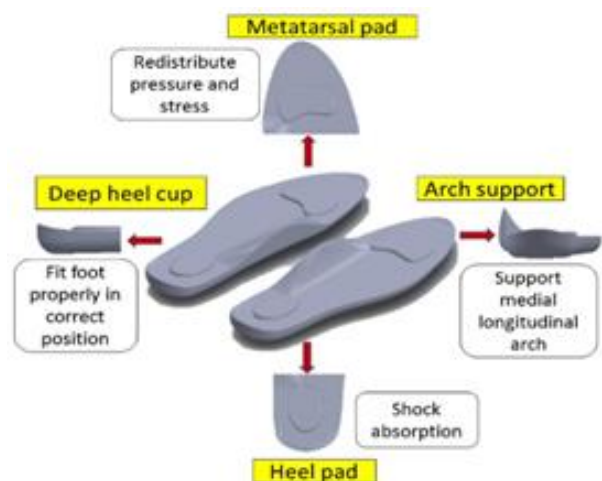

Figure 2 Characteristic of fabricated orthotic insole.

Figure 3 Fabrication of orthotic insole.

Figure 4 Fabricated insole with existing insole.

3. RESULTS AND DISCUSSION

Wireless sensors are set on lower limb muscles of tibialis anterior and peroneus longus muscles. EMG signal is recorded and collected via the wireless connections between the Trigno EMG sensors from Delsys and Trigno Wireless Foundation System. The Trigno EMG sensors are transmitted and gathered signals in the Trigno Wireless Foundation System. The collected data are filtered and been analysis by using time domain analysis which is the root mean square (RMS).

The RMS amplitude obtain for tibialis anterior muscle and peroneus muscle for fabricating and existing insole, each respondent portrays different value of muscle fatigue for left and right side of tibialis anterior and peroneus longus muscles. Many factors influence the muscle fatigue of the people. According to Mehta and Shortz [4], obesity may influence the alteration of muscle fiber type composition.
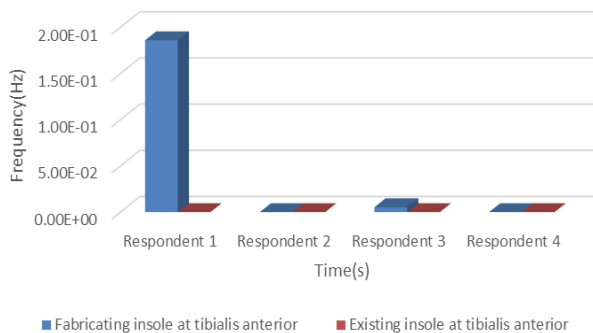

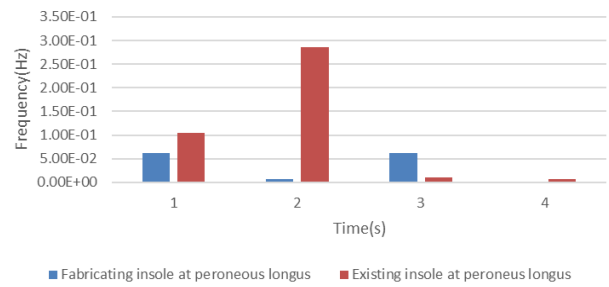
Figure 5 Average RMS amplitude on tibialis anterior muscle**.**

Figure 5 Average RMS amplitude on peroneus longus muscle.
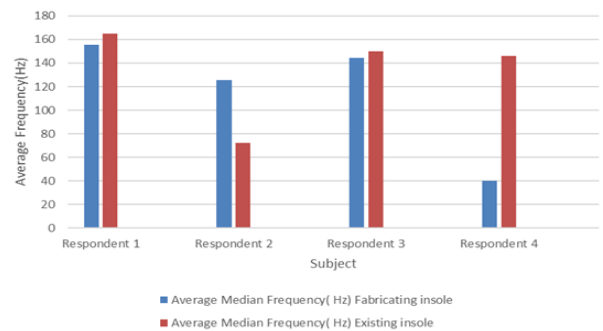

Figure 6 Average median frequency on tibialis anterior muscle**.**

Figure 7 Average median frequency on peroneus longus muscle.

4. CONCLUSION

The comparison of the measured data of electromyography (EMG) on time domain analysis with RMS amplitude and median frequency (MDF) for the fabricating insole and the existing insole showed that the fabricating insole is suitable and give slightly better performance compared to the existing insole, thus the objective of the study is achieved.

REFERENCES
[1] Brown, C. (2013). Clinical Advantage: Making Your Own Temporary Foot Orthosis. Orthopaedic Practice, (26;3:14), 204-205. Retrieved from https://www.orthopt.org/uploads/content_files/files/FASIG26.3.pdf
[2] Bateni, H. (2013). Changes of postural steadiness following use of prefabricated orthotic

insoles. *Journal of Applied Biomechanics*, *29*(2), 174-179.

[3] Mercer, J. A., & Horsch, S. (2015). Heel–toe running: A new look at the influence of foot strike pattern on impact force. *Journal of Exercise Science & Fitness*, *13*(1), 29-34.

[4] Mehta, R. K., & Shortz, A. E. (2014). Obesity-related differences in neural correlates of force control. *European Journal of Applied Physiology*, *114*(1), 197-204.

Topological optimized engine bracket for additive manufacturing

Faiz Redza Ramli[1,2,*], Zaitul Akma Said[1], Mohd Rizal Alkahari[1,3], Shafizal Mat[1,2], Mohd Nizam Sudin[1,2]

[1)]Fakulti Kejuruteraan Mekanikal, Universiti Teknikal Malaysia Melaka,
Hang Tuah Jaya, 76100 Durian Tunggal, Melaka, Malaysia
[2)]Centre for Advanced Research on Energy, Universiti Teknikal Malaysia Melaka,
Hang Tuah Jaya, 76100 Durian Tunggal, Melaka, Malaysia
[3)]Advance Manufacturing Centre, Universiti Teknikal Malaysia Melaka,
Hang Tuah Jaya, 76100 Durian Tunggal, Melaka, Malaysia

*Corresponding e-mail: faiz@utem.edu.my

Keywords: Topology optimization; 3D Printing; additive manufacturing

ABSTRACT – Engine bracket plays a crucial role in the design of an aircraft where the bracket mass directly influences the performance of aircraft. The objective of this paper is to obtain a fully optimized lightweight of engine bracket design with capability to withstand the load of the engine by using topology optimization technique and to identify the target specification baseline in terms of raw material mass, support material mass and printing time of additive manufacturing. Two topology optimization engine designs were studied by using *SolidThinking Inspire*. Afterwards the optimize design was compared with 300 existing topology optimized. The mass of engine bracket has been successfully reduced by 49% from original design without sacrificing the performance. Based on the baseline, the design is acceptable with range of 75% from all the 300 existing topological design.

1. INTRODUCTION

An engine bracket is commonly fabricated by conventional manufacturing process which in general is not fully optimized either for the performance or for the mass reduction. The role of this bracket is to hold and support the weight of the aircraft engine during handling on the engine throughout the operation time. The bracket offered an opportunity for weight reduction which is directly may reduce the cost of material.

Topology optimization (TO) is a method where material is removed by response to a given sets of loads, boundary condition and constraint. Design space is important in TO where removal of material will take place. Krishna et al. [1] found that when two beams are analyzed by using TO with different design region setting, a designer can achieve both requirements of high mass reduction while maintaining the stiffness of the part. The reduction of mass by TO might affected the performance of the product as in [2], where the stiffness of the topology optimized part reduced without sacrificing its performance requirement.

TO often produced complex geometry which is not feasible to be manufactured by conventional manufacturing but maybe produced by Additive Manufacturing (AM). However, AM suffered in printing overhanging parts and AM need support material to print the design [3]. In AM, when there is an overhang part, support structure is generated when the angle between the boundary normal and the build direction

exceeds a certain threshold. Furthermore, Leary et al.[4] have studied on optimal topology for AM which is a method for enabling AM of support-free optimal structures for FDM and found that part manufacture with support-free design and no support design have lesser printing time compare to part with support. Thus, it is important to obtain a fully optimized lightweight of engine bracket design by TO technique and to propose a design based on these AM limitations.

2. METHODOLOGY

2.1 Topology Optimization

The TO process began with the GE engine bracket design and was optimized by using Solid Thinking Inspire software. The load conditions by a design space are shown in Figure 1. The original mass of the bracket is 2.1912 kg. The design spaces were divided into two which are Topology Optimization I (TO I) and Topology Optimization II (TO II). TO I design space is located at clevis arm while TO II is located at the hole.

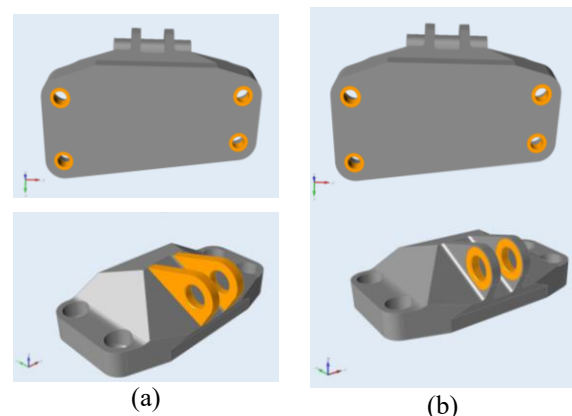|	
(a)	(b)

Figure 1 Design space for TO process in grey colour (a) TO I and (b) TO II.

There are four different load conditions which are for load condition 1 which is the 35,586 N maximum static linear of vertical load, load condition 2 which is 37,810 N maximum static linear of horizontal load, load condition 3 for maximum static linear of 42,258 N of 42 degrees from vertical and torsional load of 564 Nm at the intersection of centreline of pin and midpoint between clevis arms. In addition, supports at the bolt location are added as the rotation is allowed. The

element size and thickness constraints are auto generated which are 0.0026162 m and 0.00762 m respectively. Analysis on the stiffness was conducted on the topology optimized design in order to ensure that the von Mises stress do not violate the 903 MPa of material yield strength used which is Ti-6Al-4V by using the same load conditions.

2.2 Analysis on Target Specification Baseline

300 existing topology optimized designs of engine backet were analyzed by using FDM software in term of raw material mass, support material mass and printing time needed to be manufactured by AM.

3. RESULTS AND DISCUSSION
3.1 Topology Optimization Results

Figure 2 shows the result of TO process on engine bracket for both design spaces applied. It is shown that a lot material has been removed from the original design.
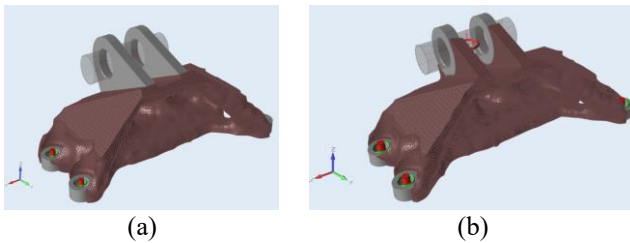

(a)   (b)

Figure 2 Topology optimized design of engine bracket (a) TO I and (b) TO II.

Table 1 shows the comparison for von Mises stress and mass for original design, topology optimized design from TO I and topology optimized design from TO II of engine bracket. As a result, TO I was accepted since the von Mises stresses for all load conditions did not exceed 903 MPa of material yield strength.

Table 1 Comparison for von Mises stress and mass for original design, TO I and TO II.

Design of engine bracket	Von Mises Stress (MPa)				Mass (kg)
	Load condition				
	1	2	3	4	
Original	677.6	477.3	530.4	771.0	2.191
TO I	819.3	510.3	579.4	886.6	1.041
TO II	824.6	537.7	589.2	916.0	1.015

3.2 Analysis on Target Specification Baseline

Topology optimized design from TO I was analyzed by FDM software for the AM output and plotted on the graph for baseline target specification. From the graph of support material mass against raw material mass as shown in Figure 3 and Figure 4, TO I showed 49% reduction of raw material mass needed to be manufactured by AM from the original design. However, there was support material mass needed for TO I. A modification was performed in order to achieve both constraints for TO and AM.

4. CONCLUSION

Topology optimization on engine bracket has reduced the mass by 49% from original design without sacrificing the performance. Based on the baseline, TO I
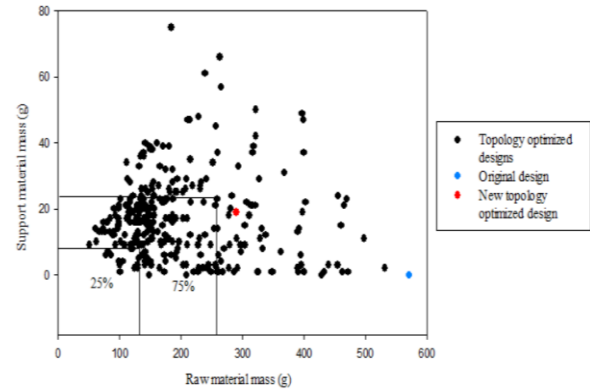
is acceptable with range of 75%.

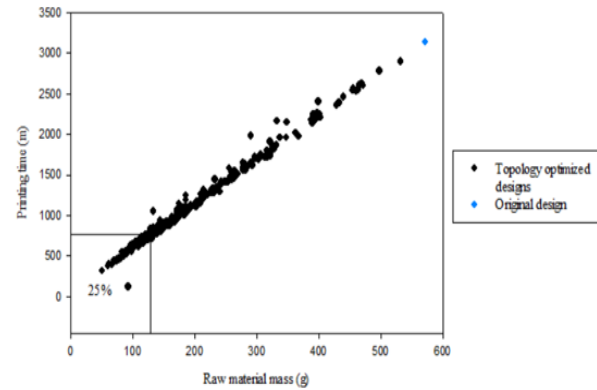Figure 3 Support material vs raw material mass.

Figure 4 Printing time vs raw material mass.

REFERENCES

[1] Krishna, L. S. R., Mahesh, N., & Sateesh, N. (2017). Topology optimization using solid isotropic material with penalization technique for additive manufacturing. *Materials today: proceedings*, *4*(2), 1414-1422.

[2] Sudin, M. N., Tahir, M. M., Ramli, F. R., & Shamsuddin, S. A. (2014). Topology optimization in automotive brake pedal redesign. *International Journal of Engineering and Technology (IJET)*, *6*(1), 398-402.

[3] Nazan, M. A., Ramli, F. R., Alkahari, M. R., Sudin, M. N., & Abdullah, M. A. (2017). Process parameter optimization of 3D printer using response surface method. *ARPN Journal of Engineering and Applied Sciences*, *12*(7), 2291-2296.

[4] Leary, M., Merli, L., Torti, F., Mazur, M., & Brandt, M. (2014). Optimal topology for additive manufacture: A method for enabling additive manufacture of support-free optimal structures. *Materials & Design*, *63*, 678-690.

Modeling and fabrication of protective mask with high complexity pattern using low-cost additive manufacturing design tool and systems

Syahibudil Ikhwan Abdul Kudus[1,3,*], Ahmad Afiq Baharuddin[1], Mastura Mohammad Taha[1,3],
Mohammad Rafi Omar[1,3], Mohd Idain Fahmy Rosley[1,3], Shafizal Mat[2,3]

[1] Fakulti Teknologi Kejuruteraan Mekanikal & Pembuatan, Universiti Teknikal Malaysia Melaka,
Hang Tuah Jaya, 76100 Durian Tunggal, Melaka, Malaysia
[2] Fakulti Kejuruteraan Mekanikal, Universiti Teknikal Malaysia Melaka,
Hang Tuah Jaya, 76100 Durian Tunggal, Melaka, Malaysia
[3] Centre for Advanced Research on Energy, Universiti Teknikal Malaysia Melaka,
Hang Tuah Jaya, 76100 Durian Tunggal, Melaka, Malaysia

*Corresponding e-mail: syahibudil@utem.edu.my

ABSTRACT – This study explores the capability to produce a complex 3-dimensional (3D) modeling using Computer Aided Design (CAD) software in combination with Additive Manufacturing (AM) systems to design and manufacture a protective mask. This study aims to produce a high complexity design pattern on the customised protective mask. The 3D modeling of the protective mask was made using AM-enabled CAD software. The protective mask was manufactured using three types of AM printers, and the 3D printed products were compared. The comparative study indicated that the presented approach offers a feasible alternative to the current practices.

1. INTRODUCTION

The application of Additive Manufacturing (AM) in wearables and assistive device has been widely recognised. AM has been used to manufacture custom-fitting medical devices such as facial prosthetics and implants directly from 3D CAD data. AM is a process of joining materials layer-by-layer to make parts from 3D CAD data [1]. The main benefit of AM in product designs is that it allows geometrical freedom, thus, create possibilities for customisation, increased product functionality, and greater complexity in manufacturing objects.

A protective mask is an item designed to protect portions of the wearer's face, including nose and eyes area from contact with objects. It must comply specific requirements that are comfort, light, and easy to use. Most protective mask were manufactured using solid polymeric materials, such as polycarbonate. There are several problems arise from the existing design of the protective mask. The solid design of existing mask lacks ventilation causing users to feel uncomfortable, thus contributes to perspiration and odour issues [4,5]. Moreover, the weight of the protective mask also have implication on the user as it provide loads on the users' face.

The unique capabilities of AM and the existence of AM-enabled CAD software (e.g., Autodesk Meshmixer) provide opportunities to improve product performance and lowering overall manufacturing cost. By adapting high complexity pattern in the product such as Voronoi, the protective mask would not only look attractive, but also improve skin ventilation and reduce weight [3].

2. METHODOLOGY

Two tasks have been carried out to develop the protective mask: (i) modeling of the protective mask – aimed to obtain the 3D data of the protective mask, and (ii) fabrication process – experimented use of AM printing system.

For the first task, the 3D modelling data of the protective mask design was obtained from the standard mannequin face and has been manipulated using Autodesk Meshmixer CAD software. For the second task, three types of 3D printing machine were used to fabricate the design. They are Up! Plus, Flashforge Creator Pro, and Projet 1000.

Up! Plus and Flashforge Creator Pro are Fused Deposition Modeling (FDM) types of machines that used material extrusion technology to fabricate the part. Acrylonitrile butadiene styrene (ABS) and polylactic acid (PLA) thermoplastic filament were used for those machines respectively. On the other hand, Projet 1000 is a Digital Light Processing (DLP) type of machine that used vat-photopolymerisation technology. Photopolymer resin was used to build the part. The process workflow of the protective mask is shown in Figure 1 below.
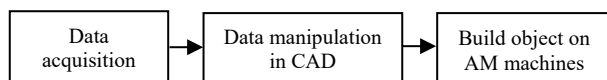

Figure 1 The process workflow [3].

During data acquisition, the measurement of the mannequin head is not precise, but rather general in length, width and height. Therefore, it needs to be dimensioned according to the real measurement of the human head. The face model wireframe was re-meshed so that the mesh triangle become smaller and denser. This step was taken in order to enable the selection process of face area that subjected to make the protective mask easier. The face is then being selected, and the size and shape of the protective mask design were determined. This step was crucial in order to establish the base of the protective mask 3D modeling. The selected mesh triangle is shown in Figure 2.
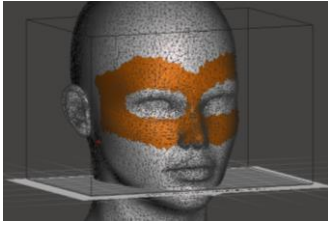
Figure 2 Selected mesh triangle on the face model.

The selected area of the protective mask then were offsets so that it provides a gap between the inner surface of the protective mask and the face. This provides airflow and space between the protective mask and the face. The selected area then was extruded to produce solid part. The thickness of the part is essential since it affects the overall condition of part weight, time taken to fabricate, and the minimum thickness requirement of the AM machines. The extruded part of the selected area also produces slight sharp edges. Therefore, smoothing those edges was performed (see Figure 3),
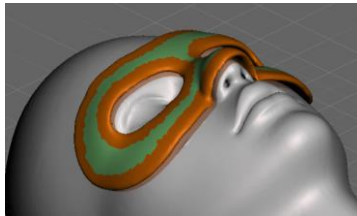

Figure 3 Smoothened mask area

The final step was applying a pattern on the protective mask design. The Voronoi pattern has been chosen to be applied to the design (see Figure 4). Nevertheless, the durability of the mask needs to be considered during this process. The 3D model data then were exported to *.STL file and printed using 3D printing machines stated above.
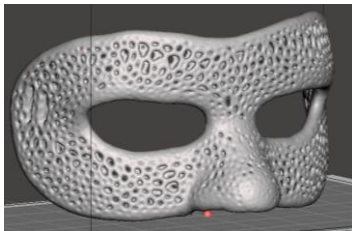

Figure 4 The protective mask with Voronoi pattern

3. RESULTS AND DISCUSSION

Table 1 shows the finished protective mask with Voronoi pattern on it and was compared based on printing time, weight, dimension and part cost. As in Table 1, it can be seen that all types of machines used in the study are capable of producing a part with high complexity pattern. All machines fabricate exact size according to original dimensions as produced in Meshmixer.

Part fabricated using Flashforge Creator Pro takes the longest time of 31 hours to produce. This was due to slow printing time, but it provides superior in detail and finishing. It produces the lightest weight and the cheapest cost amongst all. On the other hand, part fabricated using Projet 1000 has the greatest weight of 89 grams. The result also clearly shows that part produced by Projet

1000 has the highest part cost of RM176.95. Projet 1000 also is the best machine to fabricate the protective mask in terms of finishings, but the user need to adapt with the heavier part. Part printed from Up! Plus, has almost equal printing time with Projet 1000, but observation shows that it has the worst surface finish. It also heavier and costlier compared to Flashforge Creator Pro.

Table 1 Printed protective mask.

Printer type	Part	Material	Printing time	Weight (g)	Dimension (mm)	Cost (RM)
Up! Plus		ABS	10 hours	73	159.8 x 90.7 x 90.9	4.20
Flashforge Creator Pro		PLA	31 hours	60	159.8 x 90.7 x 90.9	3.27
Projet 1000		Resin	9 hours	89	159.8 x 90.7 x 90.9	176.95

4. CONCLUSION

In conclusion, designing and fabricating the protective mask from AM-enabled tool and system is fairly a straightforward process. The concept of using AM to fabricate such product is not new, but the ability to utilise the tool and systems is crucially important. Various techniques on handling CAD software has been learned in order to produce the CAD model that meets the requirements. The use of Meshmixer as a design tool to create high complexity pattern have made a significant contribution to the design and fabrication process. The selection of printing machine is also crucial because different machine produces different characteristics (e.g., visual), process capabilities (e.g., accuracy) and product costs.

REFERENCES

[1] ISO/ASTM International (2016). ISO/ASTM 52900: Standard Terminology for Additive Manufacturing Technologies. Retrieved from https://www.sis.se/api/document/preview/919975/

[2] [2] Baronio, G., Volonghi, P., & Signoroni, A. (2017). Concept and Design of a 3D Printed Support to Assist Hand Scanning for the Realization of Customized Orthosis. *Applied Bionics and Biomechanics*, 2017, 8 pages.

[3] [3] Paterson, A. M., Donnison, E., Bibb, R. J., & Campbell, R. I. (2014). Computer-aided design to support fabrication of wrist splints using 3D printing: A feasibility study. *Hand Therapy*, *19*(4), 102–113.

Solution for pes planus discomfort using corrective personalized orthotic insole via additive manufacturing

Zulkeflee Abdullah[1,2,*], Mariam Md Ghazaly[3], Azlinda Muhamad[4], Mawaddah Haslyanti[1], Mohd Amran Md Ali[1], Mohd Shahir Kasim[1], Mohammad Kamil Sued[1]

1) Fakulti Kejuruteraan Pembuatan, Universiti Teknikal Malaysia Melaka,
Hang Tuah Jaya, 76100 Durian Tunggal, Melaka, Malaysia
2) Advanced Manufacturing Centre, Universiti Teknikal Malaysia Melaka,
Hang Tuah Jaya, 76100 Durian Tunggal, Melaka, Malaysia
3) Fakulti Kejuruteraan Elektrik, Universiti Teknikal Malaysia Melaka,
Hang Tuah Jaya, 76100 Durian Tunggal, Melaka, Malaysia
4) Politeknik Muadzam Shah, 26700 Muadzam Shah, Pahang, Malaysia

*Corresponding e-mail: zulkeflee@utem.edu.my

Keywords: Additive manufacturing; pes planus; orthotics insole

ABSTRACT – This paper discussed the solution for pes planus discomfort using corrective personalized orthotic insole via additive manufacturing. The process starts from Pes Planus Screening, 3D reconstruction and foot modification. The optimization of the 3D printing process was evaluated by determining the suitable method, tools and material used when using Thermoplastic Polyurethane (TPU), a type of flexible material. TPU is difficult to print, therefore the optimized process of the FDM machine need to be determined in order to produce the customize insole. The finding shows that this new method of printing customize insole using TPU is faster, and more cost effective.

1. INTRODUCTION

Pes planus affects 20-25% of adult population word wide which causes bone structure changes and joint disorders. Pes planus also creates strained muscles and discomfort to patients. Foot orthotic devices are designed to support, correct the deformities and improve the movement of joints or limbs. Normally, foot orthotic device such as corrective insole gets the demand from patients with foot problems. Pes Planus also known as Flat Foot is the condition in which the arch of the foot collapses, with the entire foot in contact with the ground [1]. Figure 1 shows the difference between normal foot and flat foot.

Figure 1 Normal, high arch, flat foot.

According to Jin et al. [2], there are two types of foot orthotic which are custom and off-the-shelf. Custom orthoses can fit the patient's body and perform better than off-the-shelf orthoses. Due to the large range of dimensions' characteristic for each individual, a mass production is not suitable for the custom insole productions. For this reason, it is necessary to consider another approach, such as rapid prototyping technology. According to Comoros and Baritz [3], 8.8% of the rapid prototyping technologies and additive manufacturing are used for medical industry. The rapid prototyping technologies and additive manufacturing could provide benefits in terms of production time and patient satisfaction. This report will cover the development of flat foot insole, possibility and benefit of using additive manufacturing, focusing in fused deposition modelling in producing flat foot insole.

2. METHODOLOGY

This project is designing a Customised Pes Planus (Flat Foot) Orthotic Insole Using Additive Manufacturing. This device is used to correct Pes Planus problem among human. The method and procedure for the processes starts from Pes Planus Screening by expert, Photogrammetry, 3D reconstruction and foot modification using software. Then insole 3D modelling is generated and integrated into CAD software, then printed using FDM machine. Lastly Corrective Ability Evaluation by Expert. TPU, among potential flexible material will be used (Figure 2).
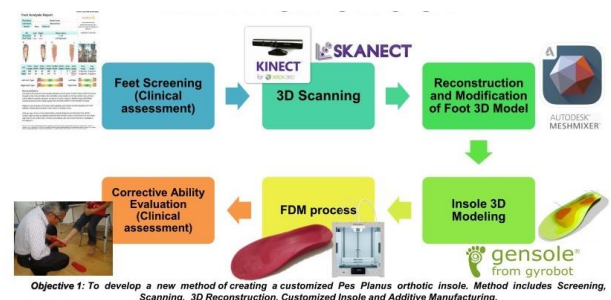

Figure 2 Steps of customized orthotic insole development process.

2.1 Feet screening

Pes Planus problem on feet and then screening by orthotics expert. Expert confirmation on the patient's feet condition of Pes Planus. Foot sensor insole was used here. Then the process of Insole sensor validation was done.

2.2 3D scanning – customized insole design

Low-cost 3D scanning solution: Microsoft® Kinect™ for XBOX 360 (gaming sensor) and our Faro Arm high end scanner at the Rapid Prototyping Lab was used to get the images. Occipital Skanect software was used to process the images.

2.3 3D reconstruction & foot modification – customized insole design

Autodesk Meshmixer software was used here. Firstly, 3D models imported from Skanect mesh, (.stl) & remove the unwanted geometry. Secondly, the details were smoothed out. Lastly, the foot alignment corrected to normal conditions. In here all problematic foot will be corrected to be a normal heathy foot according to the parameters recommended by orthotics expert.

2.4 Insole 3D Modeling – customized insole design

Gensole browser-based tool was used here. Gensole will generate insoles for 3D Printing from Gyrobot. The 3D model in .AMF files then exported into slicer for 3D printer toolpath creation.

2.5 FDM process (TPU)

FDM process parameters will be used in the study. Determination of parameters to be used in the FDM process is based on the optimum value obtained from the literature reviews.

2.5 Corrective ability evaluation

Expert confirmation on the patient's feet condition of Pes Planus. Patient has been asked to position their foot so that the plantar surface takes the normal disposition. The corrective ability of the orthotic insole has been assessed by experts to ensure the reliability of the results obtained. Experts are positive on the resulted insole provide optimal foot correction effects.

3. RESULTS AND DISCUSSION

The solution for pes planus (flat-foot) discomfort using corrective personalized orthotic insole using additive manufacturing process was verified in the previous section and has given good results. For validation of the customize insole, each patient has been certified to have a pes planus problem by an orthopaedist practitioner. At the 3D scanning stage, the 3D scanning was performed using Kinect™ for XBOX 360 (Microsoft®) paired with Skanect software as a low-cost solution. The results show comparable images with the Faro Arm Scanner but with less images quality. At the 3D Reconstruction & Foot Modification stage, there are two phases of works conducted by using Autodesk Meshmixer ver. 3.5. First phase is reconstruction of foot model. The second phase is modification of Pes Planus foot model. The foot alignment was then corrected to normal foot conditions. Then at the Pes Planus Orthotic Insole 3D

modeling using Gensole stage, the aim is correct the Pes Planus condition in Figure 3(a) to a perfect feet condition shown in Figure 3(b). Figure 4 shows the successful customize insole 3D printed using TPU flexible material.
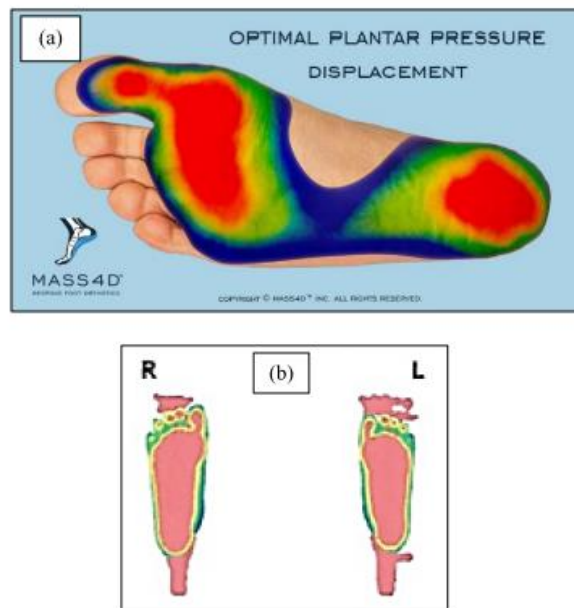

Figure 3 Pes planus vs optimal feet. (a) Feet with pes planus problem and (b) optimal foot.

Figure 4 successful customize insole 3D printed using TPU flexible material tested on patient by the orthotics expert (Dr Ahmad Tajuddin Abdullah, an Orthopedic & Traumotology Surgeon from Mahkota Orthotics and Prosthetic). Without and with personalize insole.

4. CONCLUSIONS

In conclusion, the customized pes planus (flat foot) orthotic insole using additive manufacturing was successfully verified. This study was devoted to developing customized Pes Planus orthotic insole using FDM and has the potentially contribution to the orthotic industry. The optimization was evaluated by determining the suitable method, tools and material used when using TPU flexible material. The process parameters of the FDM machine also need to be determined in order to produce the customize insole. The study showed the feasibility using low-cost 3D scan solution without compromising the quality, simplicity of using user-friendly CAD software. This study has shown that the additive manufacturing technology has the potential to be

applied in the medical industry, particularly in orthotic and prosthetic manufacturing. Future works includes clinical assessment to ensure that corrective processes are effective.

ACKNOWLEDGEMENT

REFERENCES

[1] Moorthy, T. N. & Sulaiman S. F. (2015). Individualizing characteristics of footprints in Malaysian Malays for person identification from a forensic perspective. *Egyptian Journal of Forensic Sciences*, 7, 13–22.

[2] Jin, Y. A., Plott, J., Chen, R., Wensman, J., & Shih, A. (2015). Additive manufacturing of custom orthoses and prostheses–A review. *Procedia CIRP*, *36*, 199-204.

[3] Cotoros, D. & Baritz, M. (2012). Implementing rapid prototyping technologies for corrective insoles. *International Journal of Modern Manufacturing Technologies,* IV(1)*,* 41–46.